

CHARACTERIZATION OF CRUDE OIL FOULING: DEFINING THE COKE SPECTRUM

*R. A. Shank¹ and T. R. McCartney¹

¹ 2-321 37 Ave NE, Calgary, AB, T2E 6P6, Canada; shank.roxanne@cleanharbors.com

ABSTRACT

The composition of crude oil fouling deposits in industrial processes is a complex entity. In the majority of cases, industrial operations personnel make the assumption that the hard black deposits found on heat exchangers and process lines are coke based upon visual inspection alone; however, the deposit is often far more complex.

Coke is defined as carbonaceous material; however, this does not provide sufficient information regarding the actual nature of the deposit. The chemical and physical properties of the fouling depend greatly on the hydrogen, sulphur and oxygen content, as well as the presence of co-precipitants, such as iron sulphide, asphaltenes, and salts.

More than sixty field deposits were collected and thoroughly characterized through analytical techniques, such as chemical extraction and digestion, X-Ray diffraction and X-Ray fluorescence, as well as infrared spectroscopy.

The variations in composition described for these deposits lead to the beginning of a definition of the foulant coke spectrum. This spectrum describes the wide range of physical and chemical characteristics found among coke fouling samples, and breaks it down into a few specific categories of deposit: Asphaltic, Sulfurous, Silicate and Carbonaceous, though deposits may not fall exclusively into a single category, but may be a complex mixture of several categories simultaneously.

INTRODUCTION

Crude Oil Fouling has long been a problem in oil refineries. It is costly in terms of energy efficiency, and impacts highly on the operation of the refinery. Fouling of this nature is most often identified by the operations personnel as petroleum coke when the equipment has been taken offline, or shut down, in order to clean the equipment and/or arrange for preventative maintenance to take place.

Here, a thorough characterization of a widespread array of crude oil fouling deposits from refinery equipment is presented, which serves to not only provide some keys into understanding the mechanisms and modes by which this fouling occurs, but also provides insight towards the

development of optimal cleaning methods to reduce the downtime of the exchangers and help reduce economic losses due to maintenance costs and lost production time.

Many mechanisms for the deposition of foulants from crude oil have been proposed by researchers in the field [1,2,3], and many solutions towards the mitigation and control of crude oil fouling have been offered over the past few decades [4,5,6,7]; however, the problem persists largely in part due to a misunderstanding of the issues at the operations level, as well as the pursuit of non-traditional crude streams.

Crude oil is a complex entity, and as it is heated, chemical reactions between the different species present within the feed stream may be triggered and follow various potential reaction pathways [3].

- 1) Sulfur compounds present in the oil can react with metal ions in solution leading to corrosion fouling in the form of iron sulphide [8].
- 2) Dissolved oxygen carried in the oil may react with hydrocarbon compounds through a series of autoxidation reactions leading to the formation of insoluble gums [2].
- 3) Components in the oil may undergo thermal decomposition (cracking) when temperatures are sufficiently high and over time result in the formation of coke.

Deposits collected from the refinery equipment are usually obtained after long running times [9], one to two years, and may have seen multiple different types of crude feed traveling through the system. This makes it extremely difficult to correlate the deposit chemistry with the properties of the feed material. Laboratory trials involving pilot plants have attempted to do so [10], but in terms of field deposits, the problem becomes far more complex as there are far more variables that cannot be controlled in the field [11]. Furthermore, as field deposits tend to have longer running times than laboratory deposits, the chemical and physical properties may change due to the length of time at high temperature, a process referred to as aging [12]. According to the Marsh-Griffiths model of carbon deposition, at higher temperatures, the deposit structures of hydrocarbon based fouling becomes more graphitic with aging [13].

A note regarding sample collection

A particular difficulty in heat exchanger systems is a lack of representative samples as, in many cases, the sampling cannot take place until the tubesheet has been removed from the shell. In order to adhere to many of the health and safety, and environmental requirements which surround the shutdown processes in refineries, operations teams will steam the equipment prior to opening it up to reduce the amount of volatile components that are present. This technique limits the ability of researchers to provide solid information on cleaning of heat exchanger units on-line.

Information regarding the location and collection of the deposits, as well as feedstock and operating conditions for the unit should ideally be included in the analysis

METHODS

It is important to note here, that all samples were assessed as a complete deposit. No preliminary sample preparation was performed beyond any potential steam-out processes done in the field.

Brons et al made the suggestion that the characterization of fouling deposits should be made on the toluene insoluble fraction in order to remove any trapped feedstock [14]. This technique may provide some insight into the laboratory generated fouling deposits; however, in terms of field deposits the initial extraction with toluene results in a loss of information which may be significant to the fouling process, such as concentrations of trapped paraffin and precipitated asphaltene. Thus, it is proposed here that for field-based deposits, the whole deposit should be treated as significant and only in cases where the interference with feed is obvious should this be noted and taken into account during the analysis. All assumptions on the deposit and contributions due to the feed should be left out of the equation unless the analysis warrants it.

Samples: The investigators have collected more than sixty samples of refinery fouling deposits which have been attributed as petroleum coke fouling by the operators on site. The majority of the samples are shell side fouling deposits from heat exchangers, although some samples are from preheat train furnaces, storage tanks and decoker units. Tube side heat exchanger deposits are presented alongside their shell-side counterparts (RD55A – tube side and RD55B – shell side, RD60A – tube side and RD60B – shell side), as they form part of the same unit and both sides were treated together during the cleaning process.

The first step of the characterization procedure was to assess the behavior of the deposits in the various chemical solutions: solvent extractions and acid digestions. This treatment is systematic in

nature and serves to breakdown the sample for characterization.

Organic Chemical Analysis - Solvent Extraction:

The deposit samples were crushed for homogeneity and subjected to sequential solvent extractions to determine their relative hydrocarbon content. The deposit was first placed in a solution of 99% Isopropyl alcohol (IPA) at a temperature of 80°C. The sample was then vacuum filtered, and the filtrate was placed in a freezer and allowed to cool to a temperature of -20°C to recrystallize any paraffin that may be present. The recrystallized solids were then vacuum filtered, dried and weighed.

The solids from the initial IPA digestion were collected, dried and weighed and then placed in a solution of toluene at a temperature of 130°C. The solids were collected by vacuum filtration, dried and weighed.

Analysis of the inorganic portion of the deposits was performed on the solids which remain after organic solvent extraction. This included the collection of qualitative information about the composition of the solids with Energy Dispersive X-Ray Fluorescence (ED-XRF) and the semi-quantitative data available from analysis by Powder X-Ray Diffraction (PXRD).

Powder X-Ray Diffraction and Energy Dispersive X-Ray Fluorescence:

Powder X-Ray Diffraction (PXRD) is used to identify specific crystalline compounds within the deposit. Most inorganic components present in crude oil fouling deposits (Iron Sulphide, Calcium Sulphate, Iron Oxides and Silica) will be amenable to identification by this technique, as well as some of the organic components (i.e. Graphite) although these will primarily be amorphous and thereby will not provide useable signals for identification. The secondary, or fluorescent, X-rays emitted by the material after it has been excited by the high-energy X-rays used to produce the Diffractogram, are collected and result in an Energy Dispersive X-Ray Fluorescence (ED-XRF) Spectrum which can be used for elemental analysis

All samples were analyzed on an Olympus BTX-II X-Ray diffractometer and X-Ray fluorescence spectrometer, equipped with a Cobalt (Co) X-Ray tube, after the solvent extraction stages to prevent any distortion of the spectrum from amorphous organic components. Analysis is performed by comparing the Gaussian peaks in the spectra to the wavelengths observed for the ka_1 X-Ray emission lines of elements as described by Bearden [15].

Inorganic Chemical Analysis - Acid Digestion:

After solvent extraction, the samples were subjected to sequential digestion with a series of acids. The

sample was first digested in a solution of 10% hydrochloric acid (HCl) at 60°C for 1 hour. The solids were collected through vacuum filtration, dried and weighed. Any residual solids were then digested in a solution of 15% nitric acid (HNO₃) at a temperature of 100°C for approximately 2 hours.

Finally, if any solids remained these were placed in a solution of 3% Ammonium Bifluoride and 5% Hydrochloric Acid in water (labelled as ABF:HCl going forward in this text) at a temperature of 80°C for approximately 12 hours. The filtrate was collected for further analysis by Microwave Plasma Atomic Emission Spectroscopy (MP-AES).

Microwave Plasma Atomic Emission Spectroscopy: The filtrate from each acid digestion (HCl, HNO₃, and ABF:HCl) was collected for analysis on an Agilent 4200 Microwave Plasma Atomic Emission Spectrometer (MP-AES). MP-AES, like the more commonly used Inductively Coupled Plasma Optical Emission Spectroscopy (ICP-OES), detects the elements in the solution by thermally exciting the atoms and measuring the characteristic wavelength emitted as they return to the ground state. Only specific elements were tested during this preliminary phase and included Ca, Cr, Cu, Fe, Mn, Ni, Si, Ti, V, and Zn (data not shown). Other elements will be considered in future studies, including sulphur (S), arsenic (As), magnesium (Mg), potassium (K) and sodium (Na).

Each element was assessed at two different wavelengths to ensure that any interferences from other elements in the sample were accounted for. This technique provides background regarding the dissolved components during the acid digestion, which is correlated to the PXRD and ED-XRF spectra.

Attenuated Total Reflectance Fourier Transform Infrared Spectroscopy: Attenuated Total Reflectance Fourier Transform Infrared Spectroscopy (ATR-FTIR) is used to examine the structural features of the deposits by assessing the functional group moieties described by the spectrum. Certain key frequencies are highlighted to provide insight into the nature of the chemical structure of the deposit. Furthermore, ATR-FTIR can be used to provide information regarding the aromaticity of the foulant.

The samples were analyzed as a whole (without solvent extraction or acid digestion) on an Agilent Cary 630 FTIR Spectrometer with the ATR accessory equipped with a diamond crystal. Spectra were collected with a spectral resolution of 2 cm⁻¹ and 32 scans in the 4000-650 cm⁻¹ wavenumber range.

RESULTS

The data collected from the solvent extraction and acid digestion experiments are presented together in Table 1.

Table 1. Chemical Characterization of Refinery Samples

| | Weight Percent Component (%wt) | | | | | | Solids |
|-------|--------------------------------|--------------|--------------|--------------|------------------|--------------|--------------|
| | IPA | Wax | Toluene | HCl | HNO ₃ | ABF:HCl | |
| RD01 | 2.25 | 0.63 | 4.29 | 59.75 | 9.01 | 4.36 | 19.71 |
| RD02 | 4.62 | 2.24 | 28.51 | 10.42 | 13.35 | 18.78 | 22.08 |
| RD03 | 0.45 | 0.10 | 0.78 | 2.40 | 2.19 | 2.31 | 91.77 |
| RD04 | 0.00 | 0.35 | 0.00 | 15.63 | 26.96 | 8.85 | 48.21 |
| RD05 | 0.00 | 1.73 | 56.62 | 8.54 | 1.86 | 1.82 | 29.43 |
| RD06 | 0.00 | 3.43 | 3.74 | 61.67 | 0.10 | 7.59 | 23.47 |
| RD07 | 0.00 | 0.21 | 10.86 | 4.57 | 0.00 | 6.11 | 78.25 |
| RD08 | 4.50 | 0.24 | 10.08 | 17.30 | 0.00 | - | 67.88 |
| RD09 | 7.11 | 7.92 | 84.67 | - | - | - | 0.30 |
| RD10 | 0.54 | 0.56 | 2.20 | 22.87 | 6.90 | 0.00 | 66.93 |
| RD11 | 2.19 | 0.51 | 9.08 | 4.30 | 71.35 | 1.68 | 10.89 |
| RD12 | 0.00 | 1.50 | 96.38 | - | - | - | 2.12 |
| RD13 | 0.00 | 0.12 | 0.00 | 3.68 | 0.55 | 0.00 | 95.65 |
| RD14 | 0.00 | 96.36 | 3.47 | - | - | - | 0.17 |
| RD15 | 0.00 | 0.36 | 0.00 | 19.33 | 59.52 | 7.03 | 13.76 |
| RD16 | 0.00 | 0.11 | 0.00 | 0.00 | 0.00 | 0.50 | 99.39 |
| RD17 | 5.32 | 0.12 | 7.29 | 56.72 | 13.67 | 11.38 | 5.50 |
| RD18 | 5.76 | 0.29 | 5.06 | 35.52 | 33.42 | 4.44 | 15.51 |
| RD19 | 4.45 | 0.50 | 55.96 | 4.80 | 0.00 | 5.90 | 28.39 |
| RD20 | 50.69 | 6.98 | 2.91 | 3.04 | 1.66 | 2.45 | 32.27 |
| RD21 | 9.20 | 1.80 | 84.53 | - | - | - | 4.47 |
| RD22 | 3.20 | 0.17 | 1.30 | 27.66 | 23.87 | 6.23 | 37.57 |
| RD23 | 10.41 | 0.20 | 8.36 | 0.00 | 0.00 | - | 81.03 |
| RD24 | 26.81 | 0.19 | 1.99 | 15.29 | 7.62 | 18.47 | 29.63 |
| RD25 | 14.83 | 0.09 | 9.37 | 12.57 | 9.27 | 3.05 | 50.82 |
| RD26 | 19.48 | 0.26 | 76.30 | 2.75 | 0.05 | 0.49 | 0.67 |
| RD27 | 3.01 | 0.21 | 3.48 | 1.51 | 0.83 | 7.20 | 83.76 |
| RD28 | 18.77 | 0.45 | 5.34 | 13.95 | 21.74 | 7.82 | 31.93 |
| RD29 | 0.07 | 0.10 | 1.41 | 0.49 | 6.14 | 12.66 | 79.13 |
| RD30 | 10.89 | 4.23 | 8.06 | 0.00 | 4.21 | 37.49 | 35.12 |
| RD31 | 7.76 | 0.26 | 7.38 | 14.33 | 2.02 | 10.25 | 58.00 |
| RD32 | 0.00 | 0.16 | 99.13 | - | - | - | 0.71 |
| RD33 | 0.00 | 0.13 | 0.00 | 6.79 | 1.97 | 27.68 | 63.43 |
| RD34 | 29.20 | 0.21 | 2.63 | 30.33 | 7.88 | 12.05 | 17.70 |
| RD35 | 0.00 | 0.47 | 1.49 | 25.13 | 1.45 | 12.87 | 58.59 |
| RD36 | 2.27 | 0.62 | 10.47 | 7.14 | 0.00 | 5.70 | 73.80 |
| RD37 | 0.00 | 0.08 | 0.65 | 12.18 | 5.25 | 27.76 | 54.08 |
| RD38 | 0.00 | 0.10 | 24.91 | 5.60 | 0.00 | 10.46 | 58.93 |
| RD39 | 0.03 | 0.18 | 0.38 | 1.04 | 1.71 | 0.00 | 96.66 |
| RD40 | 0.55 | 0.00 | 0.69 | 1.74 | 1.16 | 1.72 | 94.14 |
| RD41 | 31.17 | 0.90 | 12.34 | 23.18 | 27.49 | 2.38 | 2.54 |
| RD42 | 0.00 | 0.37 | 11.44 | 71.58 | 10.32 | 3.06 | 3.23 |
| RD43 | 16.56 | 0.71 | 12.93 | 55.44 | 10.66 | 2.76 | 0.94 |
| RD44 | 51.54 | 4.41 | 3.90 | 14.46 | 7.48 | 0.00 | 18.21 |
| RD45 | 13.30 | 1.35 | 79.05 | 5.27 | 0.45 | 0.34 | 0.24 |
| RD46 | 1.18 | 0.03 | 0.62 | 22.31 | 4.45 | 30.18 | 41.23 |
| RD47 | 21.20 | 2.76 | 73.71 | - | - | - | 2.33 |
| RD48 | 10.41 | 0.39 | 87.76 | - | - | - | 1.44 |
| RD49 | 7.56 | 0.42 | 5.54 | 14.76 | 10.78 | 55.01 | 5.93 |
| RD50 | 19.68 | 0.11 | 6.60 | 23.74 | 10.06 | 37.14 | 2.67 |
| RD51 | 2.73 | 0.06 | 2.16 | 4.78 | 2.14 | 3.57 | 84.56 |
| RD52 | 21.44 | 4.03 | 5.67 | 36.86 | 7.03 | 0.77 | 24.20 |
| RD53 | 39.11 | 0.15 | 1.41 | 2.23 | 7.97 | 0.00 | 49.13 |
| RD54 | 68.94 | 0.58 | 4.77 | 5.48 | 0.00 | 1.60 | 18.63 |
| RD55A | 38.91 | 1.57 | 15.02 | 23.51 | 1.37 | 5.66 | 13.96 |
| RD55B | 3.49 | 0.28 | 3.02 | 0.00 | 9.42 | 1.25 | 82.54 |
| RD56 | 0.16 | 0.27 | 0.93 | 77.59 | 1.43 | 3.25 | 16.37 |
| RD57 | 0.60 | 0.11 | 0.00 | 55.01 | - | - | 44.28 |
| RD58 | 4.64 | 0.51 | 9.50 | 31.56 | 11.93 | 3.69 | 38.17 |
| RD59 | 1.15 | 0.03 | 0.11 | 0.00 | 12.52 | 0.00 | 86.19 |
| RD60A | 6.41 | 0.21 | 44.68 | 10.98 | 22.64 | 3.95 | 11.13 |
| RD60B | 40.78 | 1.18 | 14.24 | 8.86 | 15.62 | 1.57 | 17.75 |

Values in Table 1 are given as weight% of the total sample portion which was assessed. Bolded values in Table 1 indicate which portion of the sample appears to be contributing primarily to the fouling.

The portion of the deposit which is extractable in IPA is primarily light hydrocarbons, glycol and water. Paraffin (Wax) is recrystallized from the IPA fraction. The toluene extracted portion of the deposit is primarily heavier hydrocarbons and asphaltenes. The acid digested portions of the deposit were compared against the PXRD and ED-XRF spectra, as well as the MP-AES analysis of the acid filtrate

to identify the inorganic components present. For the HCl fraction, these typically include mineral salts (NaCl, MgCl₂), iron oxides, iron sulfides, carbonates, and some sulphates. The nitric acid soluble portion includes iron polysulphides (pyrite and marcasite) and elemental sulfur. The ABF:HCl digested portion is primarily silica (SiO₂), and various silicate-based clays and silt.

Any remaining solids after the sequential solvent extractions and acid digestions are attributed to principally be insoluble amorphous carbonaceous fouling components, or coke. Further assessment of this fraction will be the subject of a future technical paper.

Powder X-Ray Diffraction PXRD and Energy Dispersive X-Ray Fluorescence ED-XRF:

ED-XRF on the Olympus BTX-II provides elemental qualification for elements found on the periodic table between sulfur (S) and selenium (Se), results are shown in Table 2, and a sample spectrum is shown for sample RD01 in Figure 1.

Only the elements which were present in the samples are indicated on the table. Cobalt (Co) is also not included in the evaluation as Co is used as the X-ray excitation source and serves as a reference for all spectra.

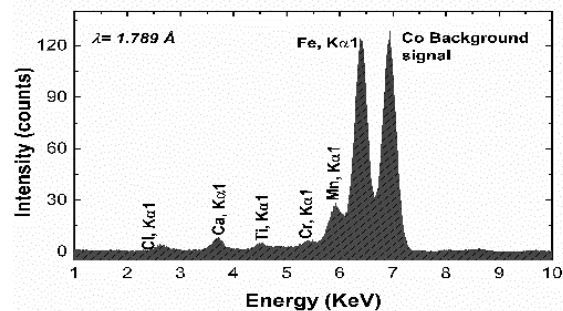


Fig. 1. Energy Dispersive X-ray Fluorescence Spectrum for the solvent extracted solid refinery deposit RD01.

PXRD is a useful tool for identifying the crystalline phases of inorganic compounds such as the type of iron sulphide scale which can be found in corrosion scale, or the metal ion inclusion that may be found in a silicate scale. The diffraction patterns, described in Table 3, obtained for the fouling deposits indicated that several different types of inorganic fouling compounds could be present. Figure 2 shows a representative PXRD pattern from sample RD55, demonstrating the complexity of the spectrum obtained even where the inorganic portion of the deposit is highly crystalline.

Any remaining solids after the sequential solvent extractions and acid digestions are attributed to principally be insoluble amorphous carbonaceous

fouling components, or coke. Further assessment of this fraction will be the subject of a future technical paper

Table 2. Measured Composition of Deposits by Energy Dispersive X-Ray Fluorescence (ED-XRF)

| | S | Cl | K | Ca | Ti | V | Cr | Mn | Fe | Ni | Cu | Zn |
|-------|---|----|---|----|----|---|----|----|----|----|----|----|
| RD01 | | x | | x | | | x | x | x | | | |
| RD02 | | | x | x | x | x | x | x | x | | x | x |
| RD03 | x | | | x | x | x | x | x | x | | | |
| RD04 | x | | | | x | | x | x | x | | | |
| RD05 | x | | | x | x | x | x | x | x | | | x |
| RD06 | x | | | x | x | x | x | x | x | | | x |
| RD07 | x | | | x | | x | x | x | x | | | |
| RD08 | | | | x | | | x | x | x | | | |
| RD09 | - | - | - | - | - | - | - | - | - | - | - | - |
| RD10 | x | | | x | | | x | x | x | | | |
| RD11 | | | | x | | | x | x | x | | | |
| RD12 | | | | x | x | | x | x | x | | | |
| RD13 | x | | | x | x | | x | x | x | | x | x |
| RD14 | - | - | - | - | - | - | - | - | - | - | - | - |
| RD15 | x | | | | | | x | x | x | | | |
| RD16 | | | | x | x | | x | x | x | | x | x |
| RD17 | | | | x | | | x | x | x | | | |
| RD18 | | x | | x | | | x | x | x | | x | |
| RD19 | | | x | x | x | | x | x | x | | x | x |
| RD20 | | | | x | x | | x | x | x | x | x | x |
| RD21 | | | | x | x | | x | x | x | | | |
| RD22 | x | | | x | | | x | x | x | | | |
| RD23 | x | | | x | | | x | x | x | | x | x |
| RD24 | | | x | x | | | x | x | x | | x | x |
| RD25 | x | | | x | | | x | x | x | | x | x |
| RD26 | x | | | x | x | x | x | x | x | | x | x |
| RD27 | x | | | x | x | x | x | x | x | x | x | x |
| RD28 | | | | | | | | x | x | | | |
| RD29 | | x | | x | | | x | x | x | | x | x |
| RD30 | | x | | x | | | x | x | x | | x | x |
| RD31 | | | | | | | x | x | x | | | |
| RD32 | - | - | - | - | - | - | - | - | - | - | - | - |
| RD33 | | | | x | | | x | x | x | | | |
| RD34 | | | | x | | | x | x | x | | | |
| RD35 | | | | | | | x | x | x | | | |
| RD36 | | | | x | x | | x | x | x | | x | x |
| RD37 | | | | x | x | | x | x | x | | | |
| RD38 | | | | x | x | | x | x | x | | x | x |
| RD39 | x | | | x | x | x | x | x | x | | x | x |
| RD40 | x | | | x | x | x | x | x | x | | x | x |
| RD41 | x | | | x | | | x | x | x | | | |
| RD42 | | | | x | | | x | x | x | | | |
| RD43 | | | | x | | | x | x | x | | | |
| RD44 | x | | | x | | | x | x | x | | x | x |
| RD45 | | | | x | x | x | x | x | x | | | |
| RD46 | | | x | | | | x | x | x | | | |
| RD47 | - | - | - | - | - | - | - | - | - | - | - | - |
| RD48 | - | - | - | - | - | - | - | - | - | - | - | - |
| RD49 | | | x | x | | | x | x | x | x | x | x |
| RD50 | | | x | x | | | x | x | x | x | x | x |
| RD51 | | | x | x | x | x | x | x | x | x | x | x |
| RD52 | | | x | | | | x | x | x | x | x | x |
| RD53 | | | x | | | | x | x | x | x | | |
| RD54 | x | | x | x | x | x | x | x | x | x | x | x |
| RD55A | | | | x | x | | x | x | x | | x | x |
| RD55B | x | | | x | x | | x | x | x | | x | x |
| RD56 | | | | x | | | x | x | x | | x | x |
| RD57 | - | - | - | - | - | - | - | - | - | - | - | - |
| RD58 | x | | | x | x | | x | x | x | | x | x |
| RD59 | | | | x | | | x | x | x | | x | x |
| RD60A | | | | | x | | x | x | x | | | x |
| RD60B | x | | | | x | | x | x | x | | | |

Powder X-Ray Diffraction PXRD and Energy Dispersive X-Ray Fluorescence ED-XRF:

ED-XRF on the Olympus BTX-II provides elemental qualification for elements found on the periodic table between sulfur (S) and selenium (Se), results are shown in Table 2, and a sample spectrum is shown for sample RD01 in Figure 1.

Only the elements which were present in the samples are indicated on the table. Cobalt (Co) is also not included in the evaluation as Co is used as the X-ray excitation source and serves as a reference for all spectra.

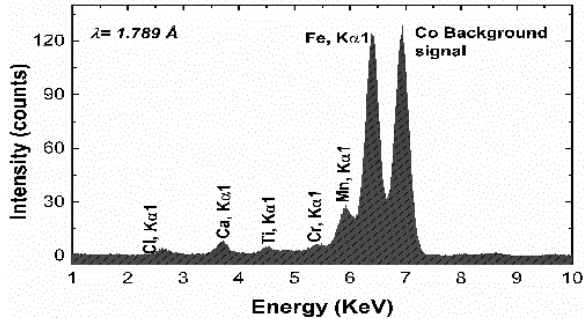


Fig. 1. Energy Dispersive X-ray Fluorescence Spectrum for the solvent extracted solid refinery deposit RD01.

PXRD is a useful tool for identifying the crystalline phases of inorganic compounds such as the type of iron sulphide scale which can be found in corrosion scale, or the metal ion inclusion that may be found in a silicate scale. The diffraction patterns, described in Table 3, obtained for the fouling deposits indicated that several different types of inorganic fouling compounds could be present. Figure 2 shows a representative PXRD pattern from sample RD55, demonstrating the complexity of the spectrum obtained even where the inorganic portion of the deposit is highly crystalline.

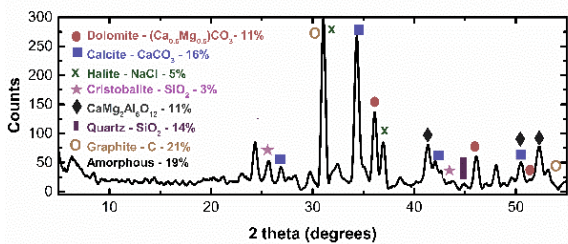


Fig. 2. Powder X-Ray Diffractogram for the solvent extracted refinery deposit RD55A. Signals corresponding to the different crystalline components are indicated according to the legend.

Common compounds include iron or metal oxides, silicates, iron sulfides, iron polysulfides and elemental sulfur, mineral salts, graphite, and occasionally raw metals or metal carbides which may have been present due to damage caused during the retrieval of the fouling deposits which can, at times, prove to be difficult to remove from the heat transfer surface manually.

Table 3. Powder X-Ray Diffraction Assignments for Refinery Deposits

| | Metal Oxide | SiO ₂ and Silicates | Salts | Metal Sulfide and Polysulfide | Elemental Sulfur | Sulphates | Carbonates and Phosphates | Graphite | Other |
|-------|-------------|--------------------------------|-------|-------------------------------|------------------|-----------|---------------------------|----------|-------|
| RD01 | 13.0 | 48.5 | 30.8 | | | | | | |
| RD02 | 1.8 | 52.3 | | | | | | | 21.0 |
| RD03 | | 29.1 | | 7.8 | 14.6 | 13.8 | | 14.0 | |
| RD04 | | 31.8 | 6.2 | 12.8 | | | 16.3 | | |
| RD05 | | 24.8 | | 11 | | | | 32.9 | |
| RD06 | | | | 9.1 | 31.9 | | | 18.9 | 5.1 |
| RD07 | 10.6 | 20.0 | | | 17.9 | 32.3 | | | |
| RD08 | 2.7 | | | | | 62.9 | | | |
| RD09 | - | - | - | - | - | - | - | - | - |
| RD10 | 15.7 | | | | 29.9 | | 11.7 | | |
| RD11 | - | - | - | - | - | - | - | - | - |
| RD12 | 2.1 | 91.3 | | 1.1 | | | | | |
| RD13 | 22.0 | | | | | | | 53.8 | |
| RD14 | - | - | - | - | - | - | - | - | - |
| RD15 | 5.7 | | | 9.3 | | 70.8 | | | |
| RD16 | 39.1 | 37.1 | | | | | | | |
| RD17 | 33.6 | 21.6 | 17.4 | | | | | | |
| RD18 | | 73.2 | | | | | | | |
| RD19 | 15.1 | 57.9 | | | | | | | |
| RD20 | | | | 2.6 | | | | 76.7 | |
| RD21 | | 93.2 | | | | | | | |
| RD22 | 3.6 | | | 25.2 | | 49.7 | | | |
| RD23 | 33.7 | 26.1 | | | | | | | |
| RD24 | 2.0 | 42.4 | | | | | 35.9 | | |
| RD25 | | | | 36.6 | | 38 | | | |
| RD26 | 28.3 | 36.4 | 8.4 | 13.6 | | | | | |
| RD27 | | 67.3 | | 12.6 | | | | | |
| RD28 | | | | 13.7 | 79.9 | | | | |
| RD29 | - | - | - | - | - | - | - | - | - |
| RD30 | - | - | - | - | - | - | - | - | - |
| RD31 | 83.1 | | | | | | | | |
| RD32 | - | - | - | - | - | - | - | - | - |
| RD33 | 5.6 | 64.5 | | 5.1 | | | | | |
| RD34 | 10.0 | 56.7 | | | | | 14.6 | | |
| RD35 | 69.8 | 22.3 | | | | | | | |
| RD36 | | 74.9 | | | | | 14.3 | | |
| RD37 | | | | | | | 56.5 | 12.5 | |
| RD38 | | 63.4 | | | | | | | |
| RD39 | | | | | 43.8 | | | 21.2 | |
| RD40 | | | | | 52.7 | | | 19.5 | |
| RD41 | | | | 75.4 | 1.6 | | | | |
| RD42 | 7.6 | 52.1 | | 3.5 | | | 9.7 | | |
| RD43 | 39.5 | 5.1 | | | | | 38.7 | | |
| RD44 | | 57.6 | 10.5 | | | | 9.8 | | |
| RD45 | | | | | 56.3 | | 32.8 | | |
| RD46 | 78.9 | | | | | | | | |
| RD47 | - | - | - | - | - | - | - | - | - |
| RD48 | - | - | - | - | - | - | - | - | - |
| RD49 | | 87.8 | | | | | | | |
| RD50 | | 52.0 | | | 12.1 | | 13.7 | | |
| RD51 | 4.6 | 54.0 | | | | | 13.1 | | |
| RD52 | - | - | - | - | - | - | - | - | - |
| RD53 | - | - | - | - | - | - | - | - | - |
| RD54 | | 86.4 | | | | | | | |
| RD55A | 10.8 | 16.6 | 5.3 | | | | 26.8 | 21.2 | |
| RD55B | - | - | - | - | - | - | - | - | - |
| RD56 | 16.9 | 53.8 | | 15.2 | | | | | |
| RD57 | - | - | - | - | - | - | - | - | - |
| RD58 | 19.3 | 47.0 | | | | | | | |
| RD59 | - | - | - | - | - | - | - | - | - |
| RD60A | | 0.8 | | 76.3 | | | | | |
| RD60B | 18.2 | | | 64.4 | | | | | |

Microwave Plasma Atomic Emission Spectroscopy: Data between wavelengths correlated well to each other, with only a few outliers that may be explained by interference with Na, As or Mg. The data obtained by MP-AES appeared to correlate quite well to that obtained by PXRD and ED-XRF, providing additional quantitative data for the elements studied.

ATR-FTIR: ATR-FTIR was used to study the functional groups present in the samples. The ATR-FTIR samples were studied as whole samples, meaning that the material in the sample was crushed and homogenized and analyzed before the solvent extraction step. The solvent extracted samples were also studied; however, the signal-to-noise (S/N) ratio for these was quite poor, making the identification of functional groups more difficult. Figure 3 shows a comparison of the solvent extracted spectrum with the whole deposit on sample number RD05, with the areas of interest highlighted. It can be seen here that the two spectra are clearly different. Thus, for consistency, only the whole deposit spectral analysis data is presented.

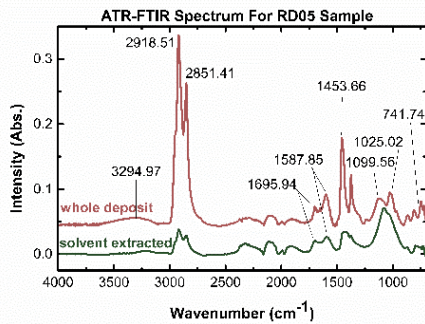


Fig. 3. Attenuated Total Reflectance Fourier Transform Infrared (ATR-FTIR) spectrum for the solvent extracted refinery deposit RD05 (green), and the whole RD05 deposit (red). Peaks of interest are highlighted on the whole deposit, as the solvent extracted deposit shows a broadening of all bands.

In order to identify the asphaltic and/or coke-like components, specific wavelengths have been considered, and only these are described in Table 4. The qualitative information is presented such that the bands are listed as low (L), medium (M) or high (H) intensity, Broad (B) or narrow (N) width.

- 3900-3100 cm^{-1} indicate the presence of $-\text{OH}$ or $-\text{NH}$ groups. Broad peaks indicate $-\text{OH}$; whereas, narrow peaks tend to indicate hydrogen bonded $-\text{NH}$ or $-\text{OH}$ groups.
- 3000-2800 cm^{-1} relates to the aromaticity of the deposit
- Around 1700 cm^{-1} represents carboxylic acid
- The 1600 cm^{-1} band is known as the coke band [9]; however, according to Fan and Watkinson (2006) this band shifts to lower wavelengths with greater aging [12]. The median wavenumber for the samples was 1580 cm^{-1} , with a standard deviation of ± 18 , suggesting aging of coke on the heat transfer surface is significant.
- 1500-1300 cm^{-1} represents alkyl stretching modes corresponding the methyl and methylene groups.
- 1100-950 cm^{-1} band region is indicative of ethers, alcohols and sulfoxides

- 1026 cm^{-1} specifically corresponds to a Carbon-Sulfur double bond ($\text{C}=\text{S}$)
- 900-700 cm^{-1} describes aromatic out-of-plane vibrations.

Table 4. Attenuated Total Reflectance Fourier Transform Infrared Spectroscopy (ATR-FTIR) Spectral Data for Refinery Samples

| | 3900-3100 -OH or -NH | 3000-2800 Arom. | 1700 -COOH | 1600 coke band | 1500-1300 alkyl | 1100-950 -O-, -OH-, S=O | 1026 C=S | 900-700 Arom. |
|-------|-------------------------|--------------------|---------------|-------------------|--------------------|-------------------------------|-------------|------------------|
| RD01 | B, M | M | - | M | M | H | - | M |
| RD02 | N, L | M | L | L, 1587 | L | H | H | M |
| RD03 | - | - | - | - | - | L | - | - |
| RD04 | B, L | L | - | L, 1617 | L | M | M | L |
| RD05 | B, L | H | L | M, 1588 | M | M | L | L |
| RD06 | B, L | H | L | M, 1588 | M | M | L | L |
| RD07 | - | L | - | L, 1572 | - | - | - | - |
| RD08 | - | M | L | L, 1588 | M | - | L | H |
| RD09 | B, M | H | - | M, 1558 | H | M | H | M |
| RD10 | B, L | M | - | M, 1580 | M | M | M | M |
| RD11 | B, L | - | L | L, 1580 | - | B, L | - | - |
| RD12 | B, L | H | L | M | M | L | L | M |
| RD13 | B, L | L | - | L, 1558 | L | L | L | L |
| RD14 | - | H | L | L, 1572 | M | L | M | - |
| RD15 | B, L | - | - | - | L | H | H | H |
| RD16 | B, L | L | L | L | L | L | - | L |
| RD17 | B, L | L | - | L, 1572 | L | H | M | M |
| RD18 | B, M | M | - | H, 1599 | H | H | H | H |
| RD19 | B, L | H | L | L, 1591 | H | L | - | H |
| RD20 | - | H | - | - | M | - | - | L |
| RD21 | B, L | M | H | H, 1580 | M | B, H | - | M |
| RD22 | B, L | L | - | - | - | B, L | L | L |
| RD23 | B, L | H | H | M, 1599 | H | H | - | M |
| RD24 | B, M | L | M | L | L | H | - | M |
| RD25 | B, L | M | - | - | L | B, M | - | M |
| RD26 | - | M | - | L, 1565 | - | B, L | - | M |
| RD27 | - | M | - | L, 1565 | L | L | L | L |
| RD28 | - | M | - | - | L | - | - | - |
| RD29 | B, M | M | - | H, 1599 | M | M | M | M |
| RD30 | B, M | M | - | H, 1543 | H | H | - | H |
| RD31 | B, M | M | L | - | M | H | M | M |
| RD32 | - | H | - | L, 1576 | M | L | - | L |
| RD33 | - | - | - | L, 1554 | - | - | - | M |
| RD34 | B, M | L | - | L, 1539 | M | H | - | M |
| RD35 | - | - | - | L, 1554 | L | - | - | M |
| RD36 | B, L | H | - | B, L, 1572 | M | - | - | M |
| RD37 | B, L | - | - | B, L, 1602 | - | L | L | - |
| RD38 | B, L | H | L | B, L, 1580 | M | M | M | L |
| RD39 | - | L | - | L, 1546 | - | - | - | L |
| RD40 | - | L | - | L, 1558 | L | L | - | L |
| RD41 | B, H | M | - | M, 1599 | M | H | H | M |
| RD42 | B, M | - | - | L, 1599 | B, M | M | - | M |
| RD43 | B, M | H | - | B, M, 1600 | M | M | M | M |
| RD44 | B, M | B, M | H | - | M | H | H | H |
| RD45 | B, L | H | - | B, M, 1576 | M | M | M | M |
| RD46 | - | L | - | - | - | - | - | L |
| RD47 | B, M | H | L | L, 1576 | M | M | L | M |
| RD48 | B, L | M | L | B, L, 1580 | L | M | M | M |
| RD49 | B, L | L | - | B, L, 1561 | L | H | - | M |
| RD50 | B, M | L | - | M, 1543 | L | H | M | M |
| RD51 | - | - | - | - | - | - | - | - |
| RD52 | B, L | M | M | B, 1591 | H | H | H | H |
| RD53 | - | - | - | - | - | - | - | - |
| RD54 | B, M | H | M | B, M, 1580 | M | M | M | M |
| RD55A | - | H | - | - | M | L | - | L |
| RD55B | B, L | H | M | M, 1584 | H | B, M | H | M |
| RD56 | - | - | - | - | - | - | L | L |
| RD57 | B, L | M | - | B, L, 1584 | M | L | L | L |
| RD58 | B, L | M | - | B, L, 1599 | M | H | H | M |
| RD59 | B, M | M | H | H | H | H | - | M |
| RD60A | B, L | H | - | B, 1565 | H | M | M | M |
| RD60B | B, L | M | - | B, 1565 | M | M | M | M |

DISCUSSION

Sixty-two deposits from refinery processes have been analyzed and presented here, all of which were identified by operations managers as coke, carbon, black stuff, or hard coke-like deposits to the researchers. A careful characterization of these field deposits identified four major categories of fouling; however, many of the deposits had components falling within more than one of these categories, and nearly a third of the samples were found to be squarely a mixture of all categories.

Category 1- Primarily Asphaltic: This category comprises the samples where the majority the deposit dissolved in the toluene extraction step. A graph of all of the samples and their toluene soluble portions is shown in figure 4. Although the toluene soluble fraction may contain heavy hydrocarbons, maltenes, and asphaltenes, it is presumed that since the deposits are all solid samples, that this fraction is highly representative of the asphaltene concentration.

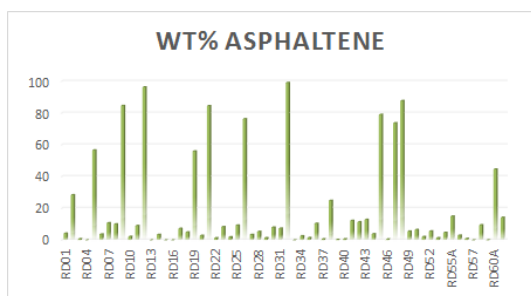


Fig. 4. The toluene soluble portion of the refinery deposits analyzed and is shown in the graph as the weight percent asphaltene.

Category 2- Primarily Sulphurous:

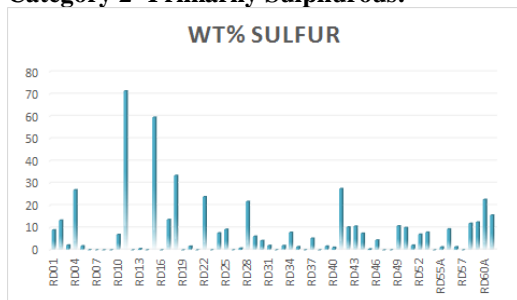


Fig. 5. The Nitric Acid soluble portion of the refinery deposits analyzed is shown in the graph as the weight percent sulphurous compounds.

Elemental sulphur and metallic polysulfide species (Me_xS_{x+1}) are not oil soluble, and are not readily dissolved by hydrochloric acid, but are readily dissolved in dilute nitric acid. Many metal sulfide species which exist in the form Me_xS_x are readily dissolved in HCl but release H_2S upon digestion. Sulphur species tend to be highly crystalline and are easily identified using PXRD. Thus, samples where the majority of the deposit was

digested during the nitric acid step, or where hydrogen sulphide was detected during the HCl digestion step, were further assessed for the presence of sulfur species in the ED-XRF spectrum and the PXRD diffractogram to confirm. A graph of all of the samples indicating % sulfurous compounds is shown in figure 5.

Category 3- Primarily Silicate: Compounds containing silica are often overlooked as being a foulant in crude oil samples. Fouling due to silica or silicate-based compounds is seen primarily in heat exchangers where the feed stocks are coming from heavy oil laden sand beds, such as those seen in the Athabasca region of Canada, or shale oil initiatives where crystalline silica is used in the hydraulic fracturing process; however, this is not exclusive.

Silica gel has been shown to undergo an aging process similar to that of coke deposits, whereby the crystal structure grows and hardens with time and temperature, often encapsulating metal ions within the unit cell [16].

The ABF:HCl soluble portion of all of the samples, attributed to silicate compounds is shown in figure 6.

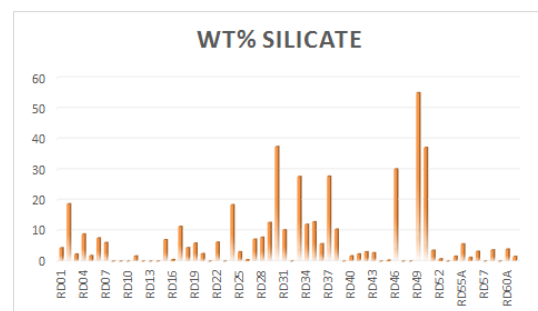


Fig. 6. The Ammonium Bifluoride: Hydrochloric Acid (ABF:HCl) soluble portion of the refinery deposits analyzed is shown in the graph as the weight percent silicate compounds.

Category 4- Primarily Amorphous Carbonaceous Material: The solid residue which remains after solvent extraction and acid digestion was assessed as being highly carbonaceous material due to its insolubility. The insoluble portion of all of the samples is shown in figure 7.

More than a third (22/62) of the samples characterized here are shown to be comprised of more than 50% of the insoluble fraction, and half of the samples are comprised of more than 30% insolubles.

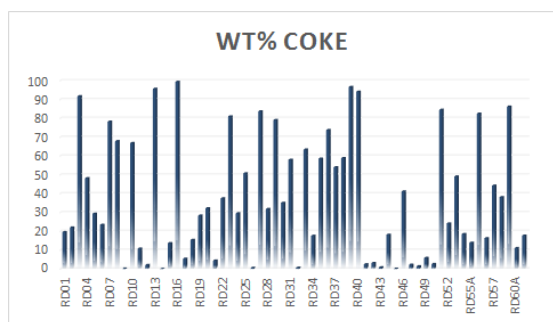


Fig. 7. The insoluble portion of the refinery deposits analyzed is shown in the graph as the weight percent carbonaceous material.

Other Components: It is important to note that other components were also observed during the characterization of these deposits. Paraffin was commonly seen in the deposits in relatively low quantities (< 2 wt%); however, in one instance it was found to be the major contributor to fouling. The hydrochloric acid soluble portion of the deposits proves to be a rather interesting fraction of the characterization process. Most of the deposits showed at least some solubility in the acid and a large portion of the samples are more than 20% soluble in HCl. The data here is compared with the data obtained through ED-XRF, PXRD and MP-AES to determine the compounds in this fraction. A portion of the compounds here are metal sulfides (troilite and mackinawite - FeS, greigite -Fe₃S₄, and pyrrhotite Fe₇S₈), a larger portion are metal oxides (magnetite - Fe₃O₄, hematite - Fe₂O₃, goethite - FeO₂, ilmenite - FeTiO₃ and some lesser metal oxides). Thus, corrosion products prove to contribute largely to the fouling in crude oil systems.

Some other compounds which contribute to this fraction are carbonates, vanadates and phosphates which were identified by PXRD and appear in Table 2. These may be artifacts from the formation and have been carried in the crude oil and deposited within the equipment.

The Coke Spectrum: Many operators simply refer to crude oil fouling as coke. The hard, black deposits collected from refinery equipment may all appear similar upon visual inspection, but without chemical characterization of the deposit it is very difficult to tell with confidence what the composition actually is. Further investigation will lead the researcher to determine that the deposit falls somewhere along the coke spectrum.

The coke spectrum was developed to help refinery operators and industrial chemical cleaning operators determine an optimal method for cleaning the deposit from the equipment. Different chemical components will require different methods of cleaning in order to return the equipment to optimal efficiency. Figure 10 depicts coke fouling as a spectrum of components, from light hydrocarbons to amorphous carbon (aka coke).

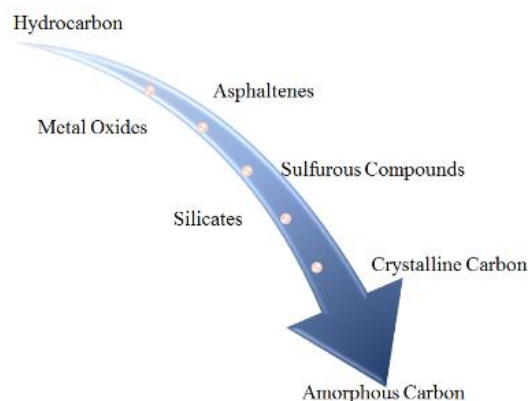


Fig. 10. The Coke Spectrum

Joshi and Brons (2003) stated it best “*Cooperative efforts are needed between refinery operators, researchers, and chemical suppliers to develop the proper solvents and to find the optimum procedures to use them for cleaning.*” [17]

CONCLUSION

Crude oil fouling in refinery production streams is often attributed to coke deposits; however, the complexity of the crude oil feedstocks and refinery operations results in the deposition of complex fouling material.

Sixty-two deposits from the field described as coke fouling were thoroughly characterized by methods such as: organic extraction, acid digestion, X-Ray Diffraction, X-Ray Fluorescence, Infrared Spectroscopy, and Atomic Emission Spectroscopy. The results of these characterizations allowed for the development of four distinct categories of deposits that are commonly associated with crude oil fouling. These are Asphaltic, Sulphurous, Silicate and Carbonaceous. Nearly a third of the deposits described here were found to be a complex mixture that had components of more than one, or all of the categories described.

Furthermore, other compounds were also found to be common co-precipitants: corrosion products, such as metal oxides and metal sulfides, as well as carbonates, vanadates and phosphates. Finally, the layering and aging of the deposits play a much larger role in field samples than those which are generated in a laboratory, and the effects of these processes should not be ignored during characterization.

The coke spectrum was developed as a reference guide for correlating cleaning applications and chemical solutions for optimal removal of the fouling deposits.

Characterization of crude oil fouling deposits is an important first step in determining optimum solutions for the chemical cleaning of refinery equipment in real world field applications. Cooperation between refinery operators, researchers, industrial chemical cleaning operators,

and chemical suppliers should be more commonplace and may lead to the development of multi-year cleaning plans which will optimize the efficiency of the refinery equipment, while reducing downtime and maintenance costs. Investigations into these applications is ongoing and will be the subject of a future article.

NOMENCLATURE

| | |
|--------------------------------|--|
| IPA | Isopropyl Alcohol |
| HCl | Hydrochloric Acid |
| HNO ₃ | Nitric Acid |
| ABF:HCl | Ammonium Bifluoride:HCl (3:5 ratio) |
| PXRD | Powder X-Ray Diffraction |
| ED-XRF | Energy Dispersive X-Ray Fluorescence |
| S/N | Signal-to-Noise Ratio |
| MP-AES | Microwave Plasma Atomic Emission Spectroscopy |
| ICP-OES | Inductively Coupled Plasma Optical Emission Spectroscopy |
| QC | Quality Control |
| ATR | Attenuated Total Reflectance |
| FTIR | Fourier Transform Infrared Spectroscopy |
| Me _x S _x | Metal Sulfide |
| wt% | percent by weight |

REFERENCES

- [1] Karabelas, A. J.; Yiantisios, S. G.; Thonon, B.; Grillot, J. M. (1997) *Appl Therm Eng*, 17(8-10), 727-737.
- [2] Watkinson, A.P. (2005) In *Proc. Int. Conf. on Understanding Heat Exchanger Fouling and Cleaning*, June 5-10, 2005. Kloster Irsee, Germany; 2005.
- [3] Coletti, F.; Crittenden, B.D.; Macchietto, S. (2015) In: *Crude Oil Fouling: Deposit Characterization, Measurements, and Modeling*. ed. Coletti, F. and Hewitt, G.F. pp. 23-50, Oxford, UK. Elsevier Inc.
- [4] Kazi, S. N. (2012) In: *Heat Exchangers – Basics Design Applications*. ed. Mitrovic, Jovan. Rijeka, Croatia. Intech Europe.
- [5] Markowski, M.; Urbaniec, K. (2005) In *Proc. Int. Conf. on Understanding Heat Exchanger Fouling and Cleaning*, June 5-10, 2005. Kloster Irsee, Germany; 2005.
- [6] Markowski, M.; Urbaniec, K. (2005) *Appl Therm Eng*. 25(7), 1019-1032.
- [7] Smaïli, F.; Vassiliadis, V. S.; Wilson, D.I. (2001) *Energy Fuels* 15(5), 1038-1056
- [8] Wang, W.; Watkinson, A. P.; (2011) In *Proc. Int. Conf. on Understanding Heat Exchanger Fouling and Cleaning*, June 5-10, 2011. Crete Island, Greece; 2011.
- [9] Venditti, S.; Berrueco, C.; Alvarez, P.; Morgan, T. J.; Millan, M.; Herod, A. A.; Kandiyoti, R.; (2009) In *Proc. Int. Conf. on Understanding Heat Exchanger Fouling and Cleaning*, June 14-19, 2009. Schlading, Austria; 2009.
- [10] Crittenden, B.D.; Hewitt, G.F.; Millan-Agorio, M.; Rostani, K.; Venditti, S.; Yang, M. (2015) *Experimental Generation of Fouling Deposits In: Crude Oil Fouling: Deposit Characterization, Measurements, and Modeling*. ed. Coletti, F. and Hewitt, G.F. pp. 51-94, Oxford, UK. Elsevier Inc.
- [11] Joshi, H. M. (2013) In *Proc. Int. Conf. on Understanding Heat Exchanger Fouling and Cleaning X*, June 9-14, 2013. Budapest, Hungary; 2013.
- [12] Fan, Z.; Watkinson, A. P.; (2006) *Ind & Eng Chem Res* 45(2006), p. 6104-6110.
- [13] Marsh, H. Griffiths, J. (1982) *Int. Symposium on Carbon Toyohashi, Japan*. Kagaku Gijutsu-sha, Tokyo.
- [14] Brons, G.; Brown, L.D.; Joshi, H.M.; Kennedy, R. J.; Bruno, T.; Rudy, T. M. (2010) United States Patent, Patent No. 7,708,864 B2, May 4.
- [15] Bearden, J. A. (1967). *Rev. of Mod. Phys.* January 1967, 86-93.
- [16] Gharaibeh, S. A.; Shank, R. A.; McCartney, T. R. (2017) In *Corrosion 2017* March 26-30, 2017. New Orleans, LA, USA. 2017-9087.
- [17] Joshi, H. M.; Brons, G. (2003) In *Proc. Int. Conf. on Understanding Heat Exchanger Fouling and Cleaning*, May 18-22, 2003. Santa Fe, New Mexico, USA; 2003.